Alma Mater Studiorum Università di Bologna
Archivio istituzionale della ricerca

A Semi-deterministic Model for Outdoor-to-Indoor Prediction in Urban Areas

(Article begins on next page)

A Semi-deterministic Model for Outdoor-to-Indoor Prediction in Urban Areas

V. Degli-Esposti, J. S. Lu, J. N. Wu, J. J. Zhu, J. A. Blaha, E. M. Vitucci, F.Fuschini, M. Barbiroli

[1]*Abstract — The prediction of indoor coverage from outdoor base stations should be of even greater interest than outdoor prediction, as most wireless data traffic is generated indoors. Due to difficulties in acquiring indoor building maps on a large scale and integrating outdoor and indoor propagation models, outdoor-to-indoor prediction has been limited in practice to the use of generic outdoor-to-indoor attenuation factors or empirical formulas. In the present work, we propose a hybrid method based on deterministic 3D outdoor prediction on building surfaces and indoor extension using a Radiosity-based iterative method that does not require a detailed building map. Prediction results are checked against measurements and, surprisingly, they appear to be almost as accurate as outdoor prediction results.*

Index Terms —Urban Propagation, Outdoor-to-indoor Propagation, Propagation Measurements, Ray Tracing, Electromagnetic scattering by random media.

I. INTRODUCTION

RF propagation in urban environment has been widely studied in the past and many propagation prediction models with different accuracy and complexity levels have been proposed [1]-[3].

Nevertheless, since indoor users - rather than outdoor ones – generate the vast majority of traffic, the accurate prediction of indoor coverage from outdoor cell sites is of particular interest for cellular manufacturers, carriers and service vendors.

Unfortunately, as indoor building maps are not easily available on a large scale and usually do not include information about construction materials and furniture, and since a combination of outdoor and indoor propagation models would be required, accurate site-specific prediction of indoor RF coverage from outdoor base stations has generally been considered impractical. Research efforts have been limited to the derivation of generic Building Penetration Loss (BPL) factors [4][5], or simple empirical formulas [6]–[9] to be combined with outdoor measurements or simple outdoor models to perform empirical-statistical indoor coverage estimates.

Recent studies have addressed accurate deterministic outdoor-to-indoor prediction using outdoor ray models combined with indoor finite-difference prediction methods [10][11], but a detailed description of the building walls and indoor structure is required for these models to work properly.

A few studies have addressed deterministic outdoor-to-indoor prediction without the use of detailed indoor building maps where ray-based outdoors prediction is performed on the buildings' outdoor walls, then either rays are propagated indoors by adding a BPL and an additional dB/m specific attenuation [12][13], or indoor prediction is achieved by switching to simple outdoor-to-indoor propagation formulas [14][15].

Indoor extension of ray-based outdoor prediction however can be dangerous due to the low spatial density of outdoor rays with respect to the limited dimensions of the indoor environment. For example, if a given strong ray illuminates only part of a building and all the other outdoor rays are weaker, by simply extending outdoor rays indoors a very uneven indoor coverage prediction might be obtained, which doesn't reflect the actual propagation process.

In this work a new approach based on the combination of a full-3D Ray Tracing (RT) outdoor model [16][17] and a simple fully-diffuse indoor propagation model, the *Radiosity Model*, is considered. While 3D RT allows for accurate prediction of the field everywhere on the outer surface of the building, the Radiosity Model accounts for the BPL and for the diffusive propagation and re-distribution of the field inside the building caused by walls, floors and furniture. Preliminary results at 850 MHz already presented in [18] are extended to a larger measurement set, which includes outdoor Above Ground Level (AGL) measurements, indoor measurements all over a high-rise building and additional 1900 MHz measurements in select buildings. Comparisons with measurements show that the Radiosity Model can realistically simulate radio wave penetration and propagation into buildings. Furthermore, the model does not degrade appreciably the outdoor prediction accuracy probably due to some sort of error-averaging effect. Lastly, results also show that different BPL values for different classes of buildings should be used to reduce the mean error.

II. MEASUREMENT DESCRIPTION

The set up used in the measurement campaigns included PCTEL Seegull LX GSM 850 MHz, Seegull LX GSM 1900 MHz, and EX Mini UMTS scanners. These scanners measure the constant radiated power from a given cell site's broadcast control channel (BCCH). All of the scanners were connected to a PCTEL OP178H omni-directional antenna with 3 dBi gain. For ground-truth position of measurement locations, a map clicker app and

GPS were used.

Two measurement campaigns were undertaken to validate the models described in Section III.

A. San Francisco Hotel measurements

The first measurement set was recorded at a hotel in central San Francisco (see Fig. 1(a)). The hotel is approximately 125 m tall and spans 2 connected buildings. To understand the radio wave propagation to the surfaces of the buildings and the subsequent propagation indoors, measurements of the received power from nearby cell sites were recorded outdoors on balconies and indoors in the public hallways and in several rooms. These measurements were recorded on almost all floors, so as to consider the different propagation effects below and above the average building heights in the vicinity. An overlay of the measurement locations inside the hotel is also plotted in Fig. 1(a).

The hotel was inside the coverage area of 8 cell sites. The base station characteristics (e.g., frequency, height, antenna type, EIRP) for each site were derived from surveying each of them. The base station heights ranged from 11 to 35 m above ground level, while their locations ranged from 250 to 1400 m from the hotel.

B. Additional Measurements

A second set of measurements was collected around and inside 4 large buildings in central San Francisco. The purpose for this collection was to separately test the Radiosity Model described later in Section III.B. All indoor and outdoor measurements were collected at Ground Level (GL). The outdoor measurements were aimed at characterizing the incident power on the outer surface of the buildings, that was used as an input to the Radiosity Model, while the indoor measurements were collected to test the accuracy of the model output on several indoor test points all over the building floor.

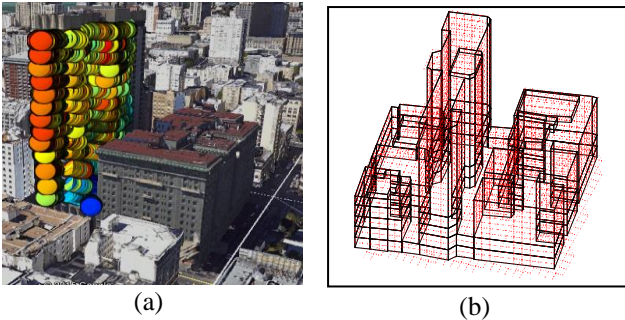(a)   (b)

Figure 1 – The considered high-rise hotel in central San Francisco: (a) aerial view with measurement locations, (b) digitized representation with tiling.

III. THE PREDICTION METHOD

To predict the field inside buildings, the proposed method first performs outdoor prediction using a full-3D RT model, and then propagates the field inside using the Radiosity Model.

A. Outdoor RT prediction

The full-3D ray tracing model described in [16][17] is used for outdoor prediction. To determine the receiver points, receiver grids over the surface of buildings are used. For example, the hotel shown in Fig. 1(a) had a receiver grid with 10 m resolution that divided the surface into 10x10m surface elements (or tiles). This resulted in a total of ~1000 receivers/outer surface tiles as shown in Fig. 1(b). Smaller rectangular tiles were used close to edges and corners to achieve a complete tessellation of the building surface. Rays were traced with a maximum of 3 reflections, 2 diffractions and 1 diffuse scattering and using the same parameters as in [17].

B. Outdoor-to-indoor prediction: the Radiosity Model

1) Background

The term *radiosity* is used in the literature to define fully diffuse back-scattering from a rough surface [19]. It has been borrowed here to identify the model described below. Here however, scattering is rather generated by building walls' surface or volume irregularities as in the Effective Roughness (ER) diffuse-scattering model [20][21]. The resulting field is the sum of a great number of contributions indirectly coming from all over the building surface, as observed in actual indoor propagation due to scattering from walls, furniture and clutter. A similar model, but applied to millimeter-wave indoor propagation, has been recently proposed in [22].

2) Algorithm

Before applying the model, also the interior of the building must be discretized. The internal volume of the building is partitioned into "virtual floors" – not necessarily coincident with the actual building floors - according to a given inter-floor distance Δh. Each floor is then subdivided into horizontal tiles so that the whole volume of the building is now filled with tiles that play the role of both scatterers and receiver points.

After discretization, the Radiosity Model diffusely propagates radio waves indoors. First, the RT-predicted fields on the tiles on the outer surface are attenuated according to the BPL L_P. For each surface (source) tile, the penetrated power flux is then scattered onto all the (destination) tiles visible to it on the same floor according to a Lambertian scattering pattern (Fig. 2(a)), as described in the sub-section below. After the power contributions coming from all source tiles are added to each destination tile, the destination tiles become source tiles. These new source tiles can forward- or backward-scatter part of their incident power as shown in Figs. 2(a)-(b). This re-scattering process is iterated using the Jacobi iteration method [23] until a maximum number of bounces off each tile N_B is met. The re-scattering direction is determined by the type of tile. For example, for the initial building penetration, forward scattering occurs for outer surface tiles. While in subsequent scattering, the destination tiles can be on the outer surface or floors/ceilings. Wall tiles backward scatter the incident field based on the reflection loss Γ of the wall. Floor/ceiling tiles can backward scatter to the same floor or forward scatter to an adjacent floor using a floor attenuation L_F.

3) Lambertian scattering and power balance

The Lambertian scattering pattern is applied in a similar way as in the ER model to preserve the power balance between reflection, transmission and scattering, but here the forward and backward scattering is fully diffuse, i.e. as with $S_R=S_T=1$ in the ER model. Also, a specific attenuation loss β [dB/m] is included on top of the free-space attenuation when propagating the field between tiles inside the building to account for excess attenuation from interior walls and clutter.

Recalling the theory in [20][21], the incident power density p_{ij} and received power P_{ij} due to backward or forward scattering on a destination "tile j" from a generic source "tile i" can be written in the form:

$$p_{ij} = \frac{P_i}{L_{P/F/R}} \frac{\cos(\theta_s)}{\pi r_{ij}^2 L_{eij}}; \qquad P_{ij} = p_{ij} \Delta A \cos(\theta_i) \tag{1}$$

where P_i is the total power impinging on source tile i, θ_s is the departing ray angle and θ_i is the incidence angle as shown in Fig. 2, r_{12} is the distance between tiles, ΔA is tile area in m^2 and $L_{e12}=10^{\wedge}(\beta\ r_{12}/10)$ is indoor excess attenuation in linear units. Also, $L_{P/F/R}$ is either the BPL, floor penetration loss or reflection loss, depending on whether the source tile i is an outer surface wall or floor tile, and whether it is forward or backward scattering.

Note that for the subsequent re-scattering where tile j becomes a source tile, the new P_i is the sum of all incident powers P_{ij} from all source tiles. Also note that when treating a tile as a receiver, the received power is the sum of powers found by summing the incident power densities multiplied by the effective receiver antenna area.
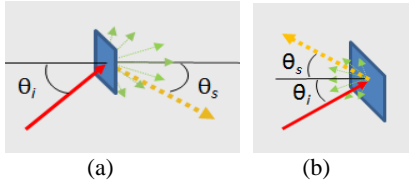

Figure 2 – (a) Forward diffuse scattering and (b) Backward diffuse scattering on a tile.

I. RESULTS

As a first step, we investigated the AGL performance of the RT model at the hotel shown in Fig. 1. Outdoor measurements were performed for 8 cell sites on balconies with above ground level heights ranging from 13 m to 103 m. An example of the RT surface predictions for cell site C41 is shown in Fig. 3(a). Mean prediction error μ_E and the error standard deviation σ_E is shown in Table I, 2nd and 3rd columns. Prediction accuracy is better than the GL results reported in [17] for the same RT model. This is not surprising as building density and cluttering are much lower in AGL conditions.

Indoor predictions were computed with the Radiosity Model using the following model's parameter values: $\Delta h=5$m, $L_P = 10$ (10 dB), $\beta=0.3$ dB/m, $\Gamma=0.2$, $L_F = 100$ (20 dB), $N_B = 5$. While Δh and N_B have been chosen according to accuracy vs. computation-time tradeoff considerations, other parameters – e.g. L_P, β, Γ and L_F - are used in other models too and values suggested in the literature for UHF frequencies have been used [6]-[9]. An example of the indoor predicted power for cell-site C41 is shown in Fig. 3(b). The corresponding error map is shown in Fig. 3(c). The error statistics for the different cell sites are reported in Table I, 4th and 5th columns. Contrary to expectations, there is little accuracy degradation despite the lack of knowledge of the internal building structure and clutter. This is probably due to the error averaging effect of the Radiosity Model, where RT prediction errors at different spots on the outdoor surface of the building are somehow averaged out by the diffusive nature of the model. As a reference, results obtained with the well-known COST 231 outdoor-to-indoor model [6] starting from the same RT prediction, are reported in the last two

columns. The following recommended parameters for the considered type of building have been used: We=10 (= L_P for comparison consistency); α=0.6; β=0.3; WGe_LOS=20; WGe_NLOS=5; Gh=0.5 [6]. It is evident that the Radiosity model peforms better than the COST 231 model, especially in terms of ID-level standard deviations: this means that its performance is more consistent over different cell-IDs.

Table I – Error statistics for the considered cell sites (850 MHz)

Cell ID [#Rx]	Outdoor AGL		Indoor (Radiosity)		Indoor (COST 231)	
	μ_E [dB]	σ_E [dB]	μ_E [dB]	σ_E [dB]	μ_E [dB]	σ_E [dB]
B83 [1680]	0.2	4.9	-6.5	5.6	-6.9	6.8
B89 [918]	3.9	7.8	-2	9.7	9.85	9.7
B9C [8036]	3.0	10.4	-6.3	10.1	-7	13.8
C2A [1352]	0.9	9.6	2.9	5.8	-0.47	5.2
C41 [9878]	4.9	6.0	5.2	8.2	0.73	7.3
C43 [6597]	-0.9	5.9	-6.3	7.7	-16.6	9.5
1A26 [2613]	2.6	9.0	-4.9	8.4	17	9.2
254F [602]	2.1	6.0	-9	9.6	-14.3	11.5
Averages	**2.1**	**7.5**	**-2.1**	**8.4**	**-4.0**	**9.6**
ID-level σ_E	**1.8**	**1.9**	**5.3**	**1.3**	**9.3**	**2.7**
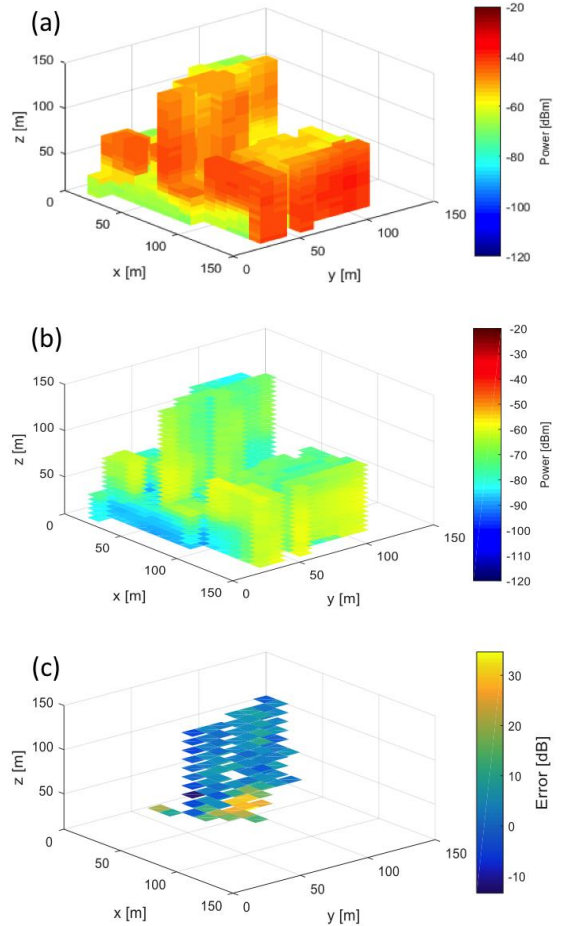
Figure 3 – (a) Prediction on the outer building surface for site C41; (b) Prediction on each Rx position/tile within the hotel; (c) Prediction error map vs. indoor measurements

For almost all cell sites the error shows a maximum with positive values for Rx locations on lower floors in the center of the building (see Fig. 3(c)). This is probably due to the walls being thicker in lower floors with respect to higher floors: better results could be obtained by varying the BPL for different floors. The mean error

appears to be negative for cell sites illuminating the building in the direction of the corridors of the high-rise section of the building (the north-south direction). This is probably due to the guiding effect of the corridors, not accounted for in the model. To improve results, the direction of the corridors could be guessed from the building shape and the indoor attenuation somehow decreased for such direction. Further investigations will be carried out on this subject.

To separately test the Radiosity Model and investigate the behavior of different buildings with different construction materials, the field measurements described in Section II.C were projected on to the outer surface tiles of the buildings and used to initialize the Radiosity Model. Indoor comparison statistics, summarized in Table II, show that while σ_E is very good, μ_E can vary from -8.1 to +3.7 dB, probably because different buildings have different BPL values. For example, one of the buildings is a shopping mall with large shopping windows at the ground floor. These windows allow for minimum outdoor to indoor attenuation, which causes a general indoor underestimation of 8 dB. The use of different BPL and β values for different building types could probably improve results.

Table II – Indoor performance for different types of buildings (1900 MHz)

Building	μ_E [dB]	σ_E [dB]
Shopping mall 1	-8.1	4.4
Shopping mall 2	3.7	5.4
Hotel	-7.3	4.4
Office building	-0.4	3.9

IV. CONCLUSIONS

In this work a new approach based on the combination of a 3D Ray Tracing (RT) outdoor model and a simple fully-diffusive radiosity-based indoor model is considered to perform outdoor-to-indoor coverage prediction. The approach is validated vs. extensive measurements in both outdoor (on the street and on balconies) and indoor cases.

Results show that: a) outdoor above-ground-level RT prediction accuracy is better than ground-level RT prediction accuracy, b) the Radiosity Model realistically describes the outdoor to indoor propagation process, c) probably due to some sort of error-averaging effect, there is little accuracy degradation in indoor prediction despite the lack of a detailed description of the indoor structure of the building, d) using a fixed 10 dB building penetration loss, mean error is quite variable with the considered building and the floor.

Result d) suggests that buildings should be divided into classes and different penetration loss values should be identified and used for different building classes and perhaps for different floors.

REFERENCES

[1] H. L. Bertoni, W. Honcharenko, L. R. Macel and H. H. Xia, "UHF propagation prediction for wireless personal communications," in Proceedings of the IEEE, vol. 82, no. 9, pp. 1333-1359, Sep 1994.

[2] M. F. Iskander and Zhengqing Yun, "Propagation prediction models for wireless communication systems," in IEEE Transactions on Microwave Theory and Techniques, vol. 50, no. 3, pp. 662-673, Mar 2002.

[3] S. Salous, V. Degli Esposti, F. Fuschini, D. Dupleich, R. Müller, R. S. Thomä, K. Haneda, J.M. Molina-Garcia-Pardo, J. Pascual-Garcia, D. P. Gaillot, M. Nekovee, S. Hur, "Millimeter-wave Propagation Characterization and Modelling Towards 5G Systems," to appear on IEEE Antennas and Propagation Magazine, December 2016.

[4] A. Davidson, and C. Hill, "Measurement of Building Penetration Into Medium Buildings at 900 and 1500 MHz," IEEE Trans. on Vehicular Technology, Vol. 46, No. 1, February 1997.

[5] F. Fuschini, M. Barbiroli, G.E. Corazza, V. Degli Esposti, G. Falciasecca, "Analysis of Outdoor-to-Indoor Propagation at 169 MHzfor Smart Metering Applications", IEEE Trans. on Ant. and Propagat., vol. 63, no. 4, April 2015, pp. 1811-1821

[6] E. Damosso and L. Correia, "Digital Mobile Radio Towards Future Generation Systems, COST 231 Final Report," European Commission, 1999.

[7] Report ITU-R M.2135-1, Guidelines for evaluation of radio interface technologies for IMT-Advanced, Dec 2009.

[8] 3GPP TR 36.873, v.1.1.1, "3rd Generation Partnership Project; Technical Specification Group Radio Accesss Network; Study on 3D channel model for LTE", 2013-09.

[9] H. Okamoto, K. Kitao, and S. Ichitsubo, "Outdoor-to-Indoor Propagation Loss Prediction in 800-MHz to 8-GHz Band for an Urban Area," Vehicular Technology, IEEE Transactions on, vol. 58, No. 3, pp. 1059– 1067, 2009.

[10] G. D. Roche, P. Flipo, Z. Lai, G. Villemaud, J. Zhang, and J. Gorce, "Implementation and validation of a new combined model for outdoor to indoor radio coverage predictions," EURASIP Journal on Wireless Communications and Networking, 2010.

[11] Y. Wang, S. Safavi-Naeini, and S. K. Chaudhuri, "A hybrid technique based on combining ray tracing and FDTD methods for site-specific modeling of indoor radio wave propagation," IEEE Trans. Antennas Propagat., vol. 48, pp. 743–754, May 2000.

[12] E. Mellios, G.S. Hilton, A.R. Nix, "Evaluating the impact of user height variations on Outdoor-to-Indoor propagation in urban macrocells and picocells using ray-tracing," in Proc. of XXXIth URSI General Assembly and Scientific Symposium (URSI GASS 2014), Beijing, China, 16-23 Aug. 2014.

[13] Y.L.C. de Jong, M.H.J.L. Koelen, M.H.A.J. Herben, "A building-transmission model for improved propagation prediction in urban microcells," IEEE Transactions on Vehicular Technology, Vol.53, No. 2, pp.490-502, March 2004.

[14] D. J. Clichon, T. C. Becker, M. Dottling, "Ray Optical Prediction of Outdoor and Indoor Coverage in Urban Macro- and Micro-Cells, in Proc. of IEEE MILCOM '96, Vol.3, pp.718-722 vol.3, 21-24 Oct 1996.

[15] F. Letourneux, S. Guivarch, Y. Lostanlen, "Propagation models for Heterogeneous Networks," in Proc. of 7th European Conference on Antennas and Propagation (EuCAP 2013), pp.3993-3997, Gothenburg, Sweden, 8-12 April 2013.

[16] F. Fuschini, E. M. Vitucci, M. Barbiroli, G. Falciasecca, V. Degli-Esposti, "Ray tracing propagation modeling for future small-cell and indoor applications," Radio Science, Volume 50, Issue 6, Pages: 469–485, June 2015.

[17] E. M. Vitucci, V. Degli-Esposti, F. Fuschini, J. S. Lu, M. Barbiroli, J. N. Wu, M. Zoli, J. J. Zhu, and H. L. Bertoni, "Ray Tracing RF Field Prediction: An Unforgiving Validation," Hindawi International Journal of Antennas and Propagation, Volume 2015, Article ID 184608, 11 pages, July 2015.

[18] V. Degli-Esposti, J. S. Lu, J. N. Wu, J. J. Zhu, J. A. Blaha, E. M. Vitucci, F.Fuschini, M. Barbiroli, "A Semi-deterministic Method for Predicting Indoor Cellular Coverage in Dense Urban Areas," 10h European Conference on Antennas and Propagation (EuCAP 2016), Davos, Switzerland, April 10-15, 2016

[19] C. Kloch and J. B. Andersen, "Radiosity—An approach to determine the effect of rough surface scattering in mobile scenarios," in Proc. IEEE Antennas and Propagation Society Int. Symp., Montreal, Canada, 1997, pp. 890–893.

[20] V. Degli Esposti, F. Fuschini, E. M. Vitucci, and G. Falciasecca, "Measurement and modelling of scattering from buildings," IEEE Trans. Antennas Propag., Vol. 55, No. 1, pp. 143–153, Jan. 2007.

[21] F. Fuschini, V. Degli-Esposti, E. M. Vitucci, "A model for forward-diffuse scattering through a wall," 4th European Conference on Antennas and Propagation, EuCAP 2010, Barcelona, Spain, 12-16 April 2010.

[22] U.-T. Virk, J.-F. Wagen and K. Haneda, "Simulating specular reflections for point cloud geometrical database of the environment," 2015 Loughborough Antennas & Propagation Conference, Loughborough University, UK, 2-3 November 2015.

[23] G. H. Golub, C. F. Van Loan, *Matrix computations*, The Johns Hopkins University Press, Third Edition, Baltimore, 1996.